Chemical Physics Letters 754 (2020) 137721

Contents lists available at ScienceDirect

Chemical Physics Letters

journal homepage: www.elsevier.com/locate/cplett

Research paper

On the search of small Cu-Ru atomically precise Superatoms. $Cu_{10}Ru$ cluster as a stable 18-*ve* endohedral structure

P.L. Rodríguez-Kessler[a,*], A.R. Rodríguez-Domínguez[b], J.A. Morato-Márquez[c], Filiberto Ortiz-Chi[d], Desmond MacLeod Carey[a], Alvaro Muñoz-Castro[a,*]

[a] Grupo de Química Inorgánica y Materiales Moleculares, Facultad de Ingeniería, Universidad Autonoma de Chile, El Llano Subercaseaux, 2801 Santiago, Chile
[b] Instituto de Física, Universidad Autónoma de San Luis Potosí, CP 78000 San Luis Potosí, México
[c] DACB-Laboratorio de Nanomateriales Catalíticos Aplicados al Desarrollo de Fuentes de Energía y Remediación Ambiental, Universidad Juárez Autónoma de Tabasco, Cunduacán 86690, Tabasco, México
[d] CONACYT-Universidad Juárez Autónoma de Tabasco, Centro de Investigación de Ciencia y Tecnología Aplicada de Tabasco, Cunduacán 86690, Tabasco, México

HIGHLIGHTS

- The $Cu_{10}Ru$ superatom with 18-ve is investigated by DFT.
- Six low-lying energy isomers with the Ru dopant inside the Cu_{10} cage are formed.
- The 17-ve counterpart Cu_9Ru, shows a large electron affinity.
- Molecular dynamics simulation confirmed the encapsulation of Ru in Cu_{10}.

ARTICLE INFO

Keywords:
Copper
Superatoms
Heteroatomic
Ruthenium

ABSTRACT

Here we discussed the plausible formation of the $Cu_{10}Ru$ cluster as a superatomic specie accounted for its $1S^21P^61D^{10}$ shell order. By stochastic structure search on $Cu_{10}Ru$ clusters, we found six low-lying cluster isomers with ΔE values from 0.0 to 4.7 kcal·mol above the ground state denoting an endohedral motif with the Ru dopant inside the Cu_{10} cage. By using molecular dynamics simulations we found a clear trend of encapsulation of the Ru atom at low temperatures. These results are useful for further rationalization and design of novel spherical superatoms expanding the libraries of stable endohedral clusters.

1. Introduction

Copper nanostructures have attracted great interest owing to their potential applications in catalysis [1–3], sensing and bioimaging [4], retaining a low-cost. In these applications, the detailed knowledge of the atomic structure of the clusters is crucial, because their physicochemical properties often depend on their shape and size [5]. Atom precise species are relevant models for rationalizing the inherent characteristics of catalytic sites, where stable clusters serve as guidance for development of new catalysts with enhanced stabilities and activities [6,7].

Recently, Cu_nRu_m alloys have shown an improved catalytic activity for hydrogen evolution reaction (HER), offering a new approach for achieving a high performance at low-cost, leading to an attractive alternative for Pt-catalysts [8]. Hence, the study of small and stable Cu_nRu_m clusters contribute to the understanding of possible catalytic sites for further rationalization and design of effective HER catalyst. Clusters holds a rich structural diversity, where certain numbers of valence electrons (*ve*) exhibit special stability, with particular presence of specific electronic shell filling, resembling to isolated atoms, and thus coined as superatoms [9]. Valence electron numbers of n = 2, 8, 18, 20, and so on, are recursive in mass spectrometric investigations [10], providing enhanced stabilities on specific clusters with a complete electronic shell [11]. In this context, the theoretical stability of different low-nuclearity systems have been reported, for Si_9Co [12], $Si_{12}Cr$ [13], and $Si_{10}Fe$ [14], denoting particularly the presence of symmetric structures such as the Frank-Kasper polyhedral cage predicted for Ti and V doped silicon clusters with at least 12 Si atoms [15,16]. From mass spectra analysis of Ag_nCo clusters, an enhanced stability peak has been observed for the $Ag_{10}Co^+$ cluster [11], provided that the Co impurity delocalize their valence 4s and 3d electrons, and each Ag atom contributes its one valence 5s electron (minus one because of the

* Corresponding authors.
E-mail addresses: rodriguezkessler.p@gmail.com (P.L. Rodríguez-Kessler), alvaro.munoz@uautonoma.cl (A. Muñoz-Castro).

https://doi.org/10.1016/j.cplett.2020.137721
Received 20 May 2020; Received in revised form 15 June 2020; Accepted 16 June 2020
Available online 17 June 2020

positive charge) what constitutes the 18-electrons complete shell. In the same manner, the theoretical stability of the neutral Ag_9Co analogue can be explained by the 18-electron rule [17]. The structures of 18-*ve* clusters such as Ag_9X (X = Fe, Co, Rh) were investigated by using structure search methods [17–19], denoting the plausible formation of polyhedral structures in clusters with different sizes. The 18-electron rule has been proposed for transition metal complexes which achieve the electronic shell closure, in which 18 electrons can fill the $s^2p^6d^{10}$ electronic configuration [20]. Therefore one can use the 18 electron rule to design superatoms involving transition metal atoms [21].

Here we pursue the stabilization of a copper cage by introducing a single dopant Ru atom achieving a favored electron count. In this work we provide an extensive exploration of the potential energy surface to identify the polyhedral structure formation of the $Cu_{10}Ru$ cluster, as a 18-ve species retaining a low dopant ratio satisfying the shell closing of the valence electrons, as expected from the superatom model. The results show the possible formation of the endohedral $Cu_{10}Ru$ cluster, which can be viewed as a Ru metal atom encapsulated inside the Cu_{10} cage. Recently, the potential applications of nanostructures have been the subject of a number of works [22–24]. In this context, the present high stability clusters are prospects for further research in building blocks of cluster-assembled nanomaterials and in molecular models of catalytic sites within Cu_nRu_m phases.

2. Computational details

Relativistic density functional theory calculations were carried out by using the ADF code [25], incorporating scalar corrections via the ZORA Hamiltonian [26]. All calculations were done employing all-electron triple-ξ Slater quality basis set, plus one polarization function (STO-TZP), within the generalized gradient approximation (GGA) namely the BP86, which includes the exchange functional of Becke [27] and the correlation functional of Perdew [28]. The BP86 approach has been previously tested for metal clusters providing results in well agreement with the experiment [29,30]. Geometry optimizations were performed without any symmetry constraint, via the analytical energy gradient method implemented by Versluis and Ziegler [31] followed by the respective vibrational analysis obtained from analytical second derivatives.

The global minimum search is performed by a stochastic approach, using the GLobal Optimization of MOlecular Systems (GLOMOS) [32], which has been found suitable for structure prediction which shows similar results compared to other methods [33–35]. The atomic positions are generated randomly by using the Mersenne twister algorithm [36]. The number of initial structures was set equal to 50 times the number of atoms in the cluster, i.e., for $Cu_{10}Ru$, the number of initial trial structures was 550. Simulated annealing (SA), based on ab-initio molecular dynamics (AIMD), is also used to corroborate the results. More details of the SA method can be found in our previous works [37,38]. Further, the performance of the computational method is tested using a range of functionals to compare the computed results with the available experimental data. The results show that the PBE0 and the B3LYP hybrid functionals overestimate the dimer bond length as shown in Table S1 (from Supplementary material), therefore the GGA approaches appear to be more reliable for predicting the geometrical parameters of these clusters. Based in the agreement between the measured data and the computational results, some GGA functionals (BP86, PBE, PW91 and B3PW91) are used to describe the equilibrium geometries for the present systems. At the BP86/TZP level, the cohesive energies of the Cu_2 and RuCu dimers found are: -58.82 kcal·mol^{-1} and -95.22 kcal·mol^{-1}, respectively, being apparently the Ru-Cu bond energetically favorable.

3. Results and discussion

To achieve the structure and electronic properties of the $Cu_{10}Ru$ cluster, first we explore the parent bare Cu_{11} cluster, which exhibits an open-shell electronic configuration with one unpaired electron. For Cu_{11} the electronic structure can be described as an incomplete filling of a 1S1P1D electronic configuration, resulting in a low symmetric structure [39]. This is given due to the 11-valence electrons of the neutral cluster does not ensure the stability of the highly symmetrical cage-like structure, as expected from the superatom model. The next favorable magic electron count is given by 18-valence electrons (*ve*) distributed in a $1S^21P^61D^{10}$ shell order [40,41]. With the aim to retain cage-like structures the only possible modification of the electron count can be introduced by doping the cage with foreign metal elements rising the available number of valence electrons to a favorable count [9]. We found that the replacement of one copper atom by Ru can effectively increase the number of cage electrons fulfilling an 18-*ve* count. Hence, ruthenium contributes with 8 electrons to the overall cluster electron count, the resulting cluster is expected to have a cage-like structure with a closed-shell (10 × Cu + Ru = 10 + 8 = 18-*ve*). The electronic structure suggest the formation of a very symmetrical polyhedral cluster with ten vertices and Ru as an endohedral atom as a tentative 18-*ve* cage displayed in Fig. 1, which have resemblance to topological modes for other cluster cage [42], allowing to have ten equivalent Cu-Ru bonds.

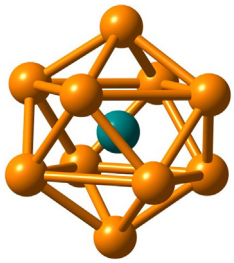

Fig. 1. Most symmetrical polyhedral cluster with 10 vertices, as a bicapped square antiprism (BSA). Color code: Cu, Orange; Ru, Green.

On the search of doped clusters the position of the metal dopant varies according to the different atomic species, e.g., for Cu_nPd clusters the Pd dopant remains in the surface site [37]. Additionally to our initial estimation of a symmetrical endohedral cage ensuring a central dopant atom embebed in a Cu_{10} cage with maximum Cu-Ru connectivity, we have performed a GLOMOS structure search strategy in order to localize the global minimum structure of the $Cu_{10}Ru$ cluster taking into account a large amount of different isomers. The obtained results by this method are further relaxed with the ADF code at the BP86/TZP level of theory.

The results from the global minima search reveal the existence of different low-lying isomers involving cake-like arrangements (Fig. 2) whereas the hypothetical BSA structure is disfavored in relation to the putative global minimum. Furthermore, all clusters are evaluated by a range of GGA functionals to determine their relative energies as shown in Table S2. The initial BSA structure (**6** isomer) with Ru in the center position on $Cu_{10}Ru$, is found to lie at 4.7 kcal·mol^{-1} above the minimum at the BP86/TZP level. Isomers 1 to 6, show endohedral structures, denoting that the Ru atom tends to be encapsulated inside the Cu_{10} cage in a range below ~5 kcal·mol^{-1} in relation to the minima, where exohedral species (isomers 7–9) are largely disfavored. The lowest energy isomer (**1**) has an endohedral structure C_{2v}-$Cu_{10}Ru$ which has a cohesion energy of about -690.37 kcal·mol^{-1}. The average Cu-Cu distance amounts 2.62 Å, which is larger than the distance found in the Cu-bulk (2.556 Å) [43], moreover, Cu-Ru distances are about of 2.47 Å slightly shorter, in agreement with previous reports of mixed Cu-Ru clusters [44]. Thus, the inclusion of Ru inside the cage is found to be more favorable than in the outside, since isomer **9** is located 57.7 kcal·mol^{-1} above the lowest structure. Other functionals show similar results (see Table S2). However since five different isomers are close in energy, we expect that these isomers are related to a

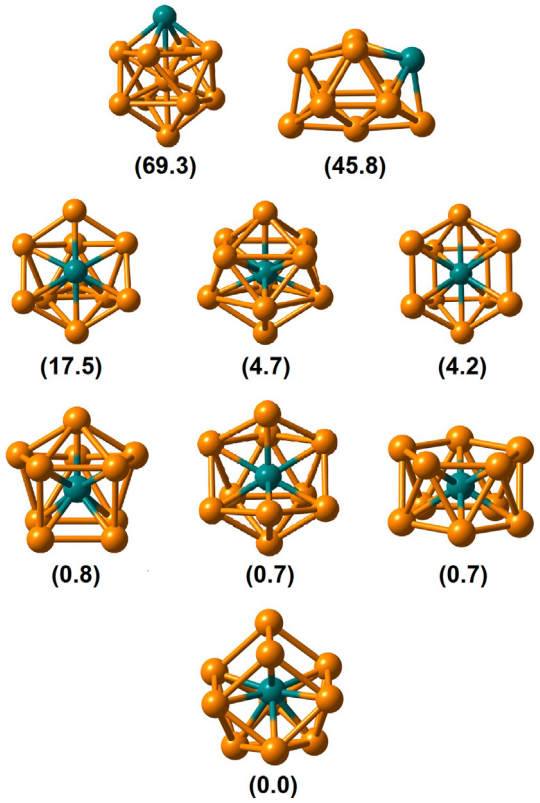

Fig. 2. Representative low-lying isomers of $Cu_{10}Ru$ clusters calculated by using the BP86/TZP level. Relative energies are given in parenthesis, values in kcal·mol^{-1}. The global minimum denoted as a C_{2v}-Ru@Cu_{10} endohedral cluster is set as reference point.

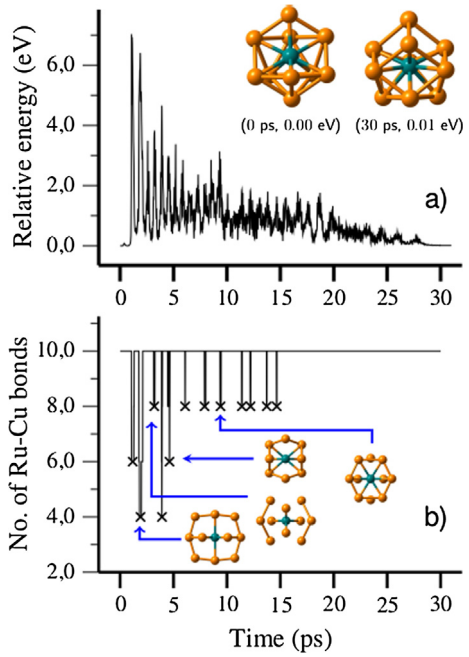

Fig. 3. (a) Relative energy versus the time step on the AIMD-SA calculation for the $Cu_{10}Ru$ cluster. (b) The number of Cu-Ru bonds during simulation.

fluxional character of $Cu_{10}Ru$ clusters, and thus can occur in the experiments (from **1** to **6**). In order to confirm result on the lowest energy structure on $Cu_{10}Ru$, we have performed a simulated annealing (SA) as shown in Fig. 3a which allows us to further collect and comment on some of the structures obtained at higher temperature denoting the calculated the number of Ru-Cu bonds on each step. In the higher temperature range of 0–15 ps we can find structures with lesser number of Ru-Cu bonds, however, in the lower temperature range between 15 and 30 ps, the structures have the highest coordination (10 Cu-Ru bonds), suggesting a clear trend for Ru encapsulation to maximize the number of Cu-Ru bonds, to increase the cluster stability. The structures found in the present work will be also confirmed with other efficient structure search methods [45–47] including different compositions of the alloy.

For **1**, the calculated HOMO-LUMO gap amounts 1.15 eV denoting a sizable frontier orbital gap compared to the classical 18-ve cluster reported by Pyykkö [WAu_{12}] [48] (1.73 eV) at the same level of theory. In order to estimate chemical stability, the electron affinity (EA) was estimated. For comparison, we recall the experimentally characterized [WAu_{12}] structure, in which the measured EA amounts to about 2.02 eV [48]. For [$Cu_{10}Ru$], the calculated AEA value of 1.26 eV (BP86/ZORA-SR) is indicative for enhanced stability slighly smaller in comparison to [WAu_{12}], which is further improved in the endohedral isomer (**6**), amounting to 2.53 eV. The adiabatic ionization potential provides further evidence for possible experimental characterization via photoelectron spectroscopy measurements, amounting to 6.30 and 6.45 eV, for **1** and **6**, which is comparable to the expected for [WAu_{12}] (6.97 eV).

Interestingly, the electron affinity calculated for the 17-ve Cu_9Ru counterpart (Fig. 4), shows a value of 2.02 eV, as an indicative of the large stabilization gained by the fulfillment of the 18-*ve* $1S^21P^61D^{10}$ electronic shell structure. This result strongly supports $Cu_{10}Ru$ as a superatom cluster, and Cu_9Ru appears as a new addition to halogen-like clusters. The electronic levels on the C_{2v}-$Cu_{10}Ru$ (**1**) structure exhibits 18-*ve* distributed on several superatomic shells accounting for 1S, 1P and 1D shells as given in Fig. 5. Hence, the binary copper-ruthenium cluster discussed here designed on the basis of the 18-*ve* principle, appears as an appropriate model for bimetallic alloys for Cu-Ru phases towards further catalyst's potential evaluation of nanostructures.

The favored endohedral $Cu_{10}Ru$ superatom is a new addition to libraries of predicted heterometallic clusters with enhanced stability, which resembles to the well known [WAu_{12}] structure [48–50], showing a related stability and a 18-*ve* electronic structure described by the $1S^21P^61D^{10}$ shell order, despite to involve the lighter copper counterpart.

4. Conclusions

In summary, we have accounted the structural stability and diversity on the $Cu_{10}Ru$ cluster isomers with a $1S^21P^61D^{10}$ electronic configuration according to the superatom approach. By exhaustive stochastic structure searches on $Cu_{10}Ru$ clusters, we found different low-lying energy isomers which exhibit a cage motif with the Ru dopant encapsulated inside a Cu_{10} cage. By using molecular dynamics simulations we further unraveled a clear trend of encapsulation of the Ru atom at low temperatures, quantified by the Cu-Ru bonds during the annealing. The global minimum structure of $Cu_{10}Ru$ has been confirmed by using a range of functional including the BP86, PW91, and B3PW91, which provided the endohedral structure formation. Lastly, the cage doping may be a useful approach for further rationalization

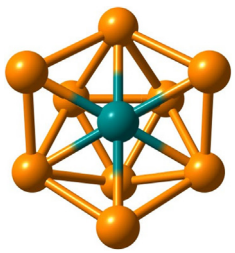

Fig. 4. Global minimum structure obtained for Cu_9Ru cluster.

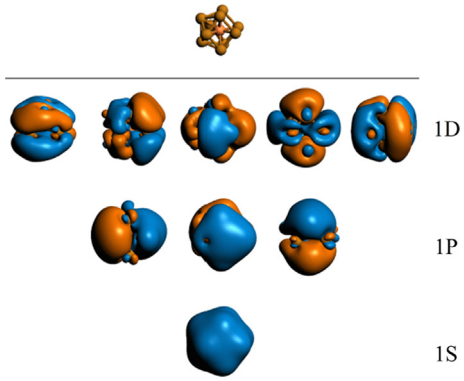

Fig. 5. Electronic levels of C_{2v}-$Cu_{10}Ru$ denoting the $1S^2\ 1P^6\ 1D^{10}$ closed-shell electronic configuration.

and design of novel spherical superatoms expanding the libraries of stable endohedral clusters. These high stability clusters are prospects for building blocks of cluster-assembled nanomaterials.

CRediT authorship contribution statement

P.L. Rodríguez-Kessler: Conceptualization, Visualization, Writing - original draft. **A.R. Rodríguez-Domínguez:** Supervision, Writing - review & editing. **Aminadat Morato-Márquez:** Investigation, Data curation. **Filiberto Ortíz Chi:** Investigation, Supervision. **Desmond MacLeod Carey:** Funding acquisition, Investigation, Supervision. **Alvaro Muñoz-Castro:** Conceptualization, Funding acquisition, Writing - review & editing.

Declaration of Competing Interest

The authors declare that they have no known competing financial interests or personal relationships that could have appeared to influence the work reported in this paper.

Acknowledgments

The authors thank the financial support from FONDECYT 1180683 and FONDECYT postdoctorado 3190329 (P. L. R.-K.). F. O.-C. thanks CONACYT (grant Al-S-26876) for financial support.

Appendix A. Supplementary material

Supplementary data to this article can be found online at https://doi.org/10.1016/j.cplett.2020.137721.

References

[1] Y. Lu, W. Chen, Sub-nanometre sized metal clusters: from synthetic challenges to the unique property discoveries, Chem. Soc. Rev. 41 (2012) 3594, https://doi.org/10.1039/c2cs15325d.
[2] N.A. Dhas, C.P. Raj, A. Gedanken, Synthesis, Characterization, and Properties of Metallic Copper Nanoparticles, Chem. Mater. 10 (1998) 1446–1452, https://doi.org/10.1021/cm9708269.
[3] W. Wei, Y. Lu, W. Chen, S. Chen, One-Pot Synthesis, Photoluminescence, and Electrocatalytic Properties of Subnanometer-Sized Copper Clusters, J. Am. Chem. Soc. 133 (2011) 2060–2063, https://doi.org/10.1021/ja109303z.
[4] B.H. Cogollo-Olivo, N. Seriani, J.A. Montoya, Unbiased structural search of small copper clusters within DFT, Chem. Phys. 461 (2015) 20–24, https://doi.org/10.1016/j.chemphys.2015.08.023.
[5] G.H. Guvelioglu, P. Ma, X. He, R.C. Forrey, H. Cheng, Evolution of Small Copper Clusters and Dissociative Chemisorption of Hydrogen, Phys. Rev. Lett. 94 (2005) 026103, , https://doi.org/10.1103/PhysRevLett.94.026103.
[6] E. Jimenez-Izal, B.C. Gates, A.N. Alexandrova, Designing clusters for heterogeneous catalysis, Phys. Today. 72 (2019) 38–43, https://doi.org/10.1063/PT.3.4248.
[7] O. Hübner, H.-J. Himmel, Metal Cluster Models for Heterogeneous Catalysis: A Matrix-Isolation Perspective, Chem. – A Eur. J. 24 (2018) 8941–8961, https://doi.org/10.1002/chem.201706097.
[8] Q. Wu, M. Luo, J. Han, W. Peng, Y. Zhao, D. Chen, M. Peng, J. Liu, F.M.F. de Groot, Y. Tan, Identifying Electrocatalytic Sites of the Nanoporous Copper-Ruthenium Alloy for Hydrogen Evolution Reaction in Alkaline Electrolyte, ACS Energy Lett. 5 (2020) 192–199, https://doi.org/10.1021/acsenergylett.9b02374.
[9] D. MacLeod Carey, A. Muñoz-Castro, $Au_{11}Re$: A hollow or endohedral binary cluster? Chem. Phys. Lett. 701 (2018) 30–33, https://doi.org/10.1016/j.cplett.2018.04.038.
[10] E. Janssens, S. Neukermans, X. Wang, N. Veldeman, R.E. Silverans, P. Lievens, Stability patterns of transition metal doped silver clusters: Dopant- and size-dependent electron delocalization, Eur. Phys. J. D. 34 (2005) 23–27, https://doi.org/10.1140/epjd/e2005-00106-9.
[11] E. Janssens, S. Neukermans, H.M.T. Nguyen, M.T. Nguyen, P. Lievens, Quenching of the Magnetic Moment of a Transition Metal Dopant in Silver Clusters, Phys. Rev. Lett. 94 (2005) 113401, , https://doi.org/10.1103/PhysRevLett.94.113401.
[12] L. Ma, J. Zhao, J. Wang, Q. Lu, L. Zhu, G. Wang, Structure and electronic properties of cobalt atoms encapsulated in Si_n (n = 1–13) clusters, Chem. Phys. Lett. 411 (2005) 279–284, https://doi.org/10.1016/j.cplett.2005.06.062.
[13] S.N. Khanna, B.K. Rao, P. Jena, Magic Numbers in Metallo-Inorganic Clusters: Chromium Encapsulated in Silicon Cages, Phys. Rev. Lett. 89 (2002) 016803, , https://doi.org/10.1103/PhysRevLett.89.016803.
[14] S.N. Khanna, B.K. Rao, P. Jena, S.K. Nayak, Stability and magnetic properties of iron atoms encapsulated in Si clusters, Chem. Phys. Lett. 373 (2003) 433–438, https://doi.org/10.1016/S0009-2614(03)00511-6.
[15] P. Claes, V.T. Ngan, M. Haertelt, J.T. Lyon, A. Fielicke, M.T. Nguyen, P. Lievens, E. Janssens, The structures of neutral transition metal doped silicon clusters, Si_nX (n = 6–9; X = V, Mn), J. Chem. Phys. 138 (2013) 194301, , https://doi.org/10.1063/1.4803871.
[16] V. Kumar, Y. Kawazoe, Metal-Encapsulated Fullerenelike and Cubic Caged Clusters of Silicon, Phys. Rev. Lett. 87 (2001) 045503, , https://doi.org/10.1103/PhysRevLett.87.045503.
[17] P.L. Rodríguez-Kessler, A.R. Rodríguez-Domínguez, Structural, electronic, and magnetic properties of Ag_nCo (n = 1–9) clusters: A first-principles study, Comput. Theor. Chem. (2015), https://doi.org/10.1016/j.comptc.2015.05.009.
[18] R. Dong, X. Chen, H. Zhao, X. Wang, H. Shu, Z. Ding, L. Wei, Structural, electronic and magnetic properties of Ag_nFe clusters (n ≤ 15): local magnetic moment interacting with delocalized electrons, J. Phys. B At. Mol. Opt. Phys. 44 (2011) 035102, , https://doi.org/10.1088/0953-4075/44/3/035102.
[19] P.L. Rodríguez-Kessler, S. Pan, E. Florez, J.L. Cabellos, G. Merino, Structural Evolution of the Rhodium-Doped Silver Clusters Ag_nRh (n ≤ 15) and Their Reactivity toward NO, J. Phys. Chem. C. 121 (2017), https://doi.org/10.1021/acs.jpcc.7b05048.
[20] S.N. Khanna, P. Jena, Assembling crystals from clusters, Phys. Rev. Lett. 69 (1992) 1664–1667, https://doi.org/10.1103/PhysRevLett.69.1664.
[21] P. Jena, Q. Sun, Super Atomic Clusters: Design Rules and Potential for Building Blocks of Materials, Chem. Rev. 118 (2018) 5755–5870, https://doi.org/10.1021/acs.chemrev.7b00524.
[22] Q. Sun, M. Wang, Z. Li, A. Du, D.J. Searles, Carbon Dioxide Capture and Gas Separation on B 80 Fullerene, J. Phys. Chem. C. 118 (2014) 2170–2177, https://doi.org/10.1021/jp407940z.
[23] Q. Sun, C. Sun, A. Du, Z. Li, Charged-Controlled Separation of Nitrogen from Natural Gas Using Boron Nitride Fullerene, J. Phys. Chem. C. 118 (2014) 30006–30012, https://doi.org/10.1021/jp510387h.
[24] Q. Sun, Z. Li, D.J. Searles, Y. Chen, G. (Max) Lu, A. Du, Charge-Controlled Switchable CO_2 Capture on Boron Nitride Nanomaterials, J. Am. Chem. Soc. 135 (2013) 8246–8253, https://doi.org/10.1021/ja400243r.
[25] Amsterdam Density Functional (ADF) Code, Vrije Universiteit: Amsterdam, The Netherlands. http://www.scm.com., (n.d.). https://doi.org/adf.
[26] E. van Lenthe, E.-J.J. Baerends, J.G. Snijders, Relativistic total energy using regular approximations, J. Chem. Phys. 101 (1994) 9783, https://doi.org/10.1063/1.467943.
[27] A.D. Becke, Density-functional exchange-energy approximation with correct asymptotic behavior, Phys. Rev. A. 38 (1988) 3098–3100, https://doi.org/10.1103/PhysRevA.38.3098.
[28] J.P. Perdew, Density-functional approximation for the correlation energy of the inhomogeneous electron gas, Phys. Rev. B. 33 (1986) 8822–8824, https://doi.org/10.1103/PhysRevB.33.8822.
[29] P.V. Nhat, N.T. Si, M.T. Nguyen, Elucidation of the molecular and electronic structures of some magic silver clusters Ag_n (n = 8, 18, 20), J. Mol. Model. 24 (2018) 209, https://doi.org/10.1007/s00894-018-3730-8.
[30] M. Harb, F. Rabilloud, D. Simon, A. Rydlo, S. Lecoultre, F. Conus, V. Rodrigues, C. Félix, Optical absorption of small silver clusters: Ag_n, (n = 4-22), J. Chem. Phys. 129 (2008), https://doi.org/10.1063/1.3013557.
[31] L. Versluis, T. Ziegler, The determination of molecular structures by density functional theory. The evaluation of analytical energy gradients by numerical integration, J. Chem. Phys. 88 (1988) 322–328, https://doi.org/10.1063/1.454603.
[32] R. Grande-Aztatzi, P.R. Martínez-Alanis, J.L. Cabellos, E. Osorio, A. Martínez, G. Merino, Structural evolution of small gold clusters doped by one and two boron atoms, J. Comput. Chem. 35 (2014) 2288–2296, https://doi.org/10.1002/jcc.23748.
[33] L. Cheng, K. Xiao-Yu, L. Zhi-Wen, M. Ai-Jie, M. Yan-Ming, Determination of Structures, Stabilities, and Electronic Properties for Bimetallic Cesium-Doped Gold Clusters: A Density Functional Theory Study, J. Phys. Chem. A. 115 (2011) 9273–9281, https://doi.org/10.1021/jp2042153.
[34] B. Chen, W. Sun, X. Kuang, G.L. Gutsev, C. Lu, Modification of Geometric and Electronic Structures of Iron Clusters by Nitrogen: Fe_8^- vs Fe_8N^-, J. Phys. Chem. C. 124 (2020) 3867–3872, https://doi.org/10.1021/acs.jpcc.9b10916.

[35] P. Li, X. Du, J.J. Wang, C. Lu, H. Chen, Probing the Structural Evolution and Stabilities of Medium-Sized $MoB_n^{0/-}$ Clusters, J. Phys. Chem. C. 122 (2018) 20000–20005, https://doi.org/10.1021/acs.jpcc.8b05759.
[36] M. Matsumoto, T. Nishimura, Mersenne twister: a 623-dimensionally equidistributed uniform pseudo-random number generator, ACM Trans. Model. Comput. Simul. 8 (1998) 3–30, https://doi.org/10.1145/272991.272995.
[37] P.L. Rodríguez-Kessler, P. Alonso-Dávila, P. Navarro-Santos, J.A. Morato-Márquez, F. Ortíz-Chi, A.R. Rodríguez-Domínguez, Hydrogen Chemisorption on Pd-Doped Copper Clusters, J. Phys. Chem. C. 123 (2019) 15834–15840, https://doi.org/10.1021/acs.jpcc.9b03637.
[38] P.L. Rodríguez-Kessler, P. Navarro-Santos, A.R. Rodríguez-Domínguez, Structural characterization of Co-doped Pd_n (n = 1–12) clusters: First-principles calculations, Chem. Phys. Lett. 715 (2018) 141–146, https://doi.org/10.1016/j.cplett.2018.11.012.
[39] A.S. Chaves, G.G. Rondina, M.J. Piotrowski, P. Tereshchuk, J.L.F. Da Silva, The role of charge states in the atomic structure of Cun and Pt_n (n = 2–14 atoms) clusters: A DFT investigation, J. Phys. Chem. A. 118 (2014) 10813–10821, https://doi.org/10.1021/jp508220h.
[40] M. Yadav, H. Fang, S. Giri, P. Jena, Ligand stabilization of manganocene dianions – in defiance of the 18-electron rule, Phys. Chem. Chem. Phys. 21 (2019) 24300–24307, https://doi.org/10.1039/C9CP02331C.
[41] J. Zhou, S. Giri, P. Jena, 18-Electron rule inspired Zintl-like ions composed of all transition metals, Phys. Chem. Chem. Phys. 16 (2014) 20241–20247, https://doi.org/10.1039/C4CP03141E.
[42] A. Lupan, A.A.A. Attia, R.B. King, Unusual dimetallaborane cluster polyhedra and their skeletal bonding, Coord. Chem. Rev. 345 (2017) 1–15, https://doi.org/10.1016/j.ccr.2016.11.001.
[43] C. Kittel, Introduction to Solid State Physics, 4th ed., Wiley Sons, New York, NY, 1971.
[44] M.A. Beswick, J. Lewis, P.R. Raithby, M.C.R. de Arellano, [Ru20H4Cu6Cl2(CO)48]4: A New High Nuclearity Copper-Ruthenium Cluster, Angew. Chemie Int. Ed. English. 36 (1997) 2227–2228, https://doi.org/10.1002/anie.199722271.
[45] B. Le Chen, W.G. Sun, X.Y. Kuang, C. Lu, X.X. Xia, H.X. Shi, G. Maroulis, Structural Stability and Evolution of Medium-Sized Tantalum-Doped Boron Clusters: A Half-Sandwich-Structured TaB_{12} – Cluster, Inorg. Chem. 57 (2018) 343–350, https://doi.org/10.1021/acs.inorgchem.7b02585.
[46] Y. Tian, D. Wei, Y. Jin, J. Barroso, C. Lu, G. Merino, Exhaustive exploration of MgB_n (n = 10–20) clusters and their anions, Phys. Chem. Chem. Phys. 21 (2019) 6935–6941, https://doi.org/10.1039/C9CP00201D.
[47] S. Jin, B. Chen, X. Kuang, C. Lu, W. Sun, X. Xia, G.L. Gutsev, Structural and Electronic Properties of Medium-Sized Aluminum-Doped Boron Clusters AlB_n and Their Anions, J. Phys. Chem. C. 123 (2019) 6276–6283, https://doi.org/10.1021/acs.jpcc.9b00291.
[48] P. Pyykkö, N. Runeberg, Icosahedral WAu_{12}: A Predicted Closed-Shell Species, Stabilized by Aurophilic Attraction and Relativity and in Accord with the 18-Electron Rule, Angew. Chemie Int. Ed. 41 (2002) 2174–2176, https://doi.org/10.1002/1521-3773(20020617)41:12<2174::AID-ANIE2174>3.0.CO;2-8.
[49] J. Autschbach, B.A. Hess, M.P. Johansson, J. Neugebauer, M. Patzschke, P. Pyykkö, M. Reiher, D. Sundholm, Properties of WAu_{12}, Phys. Chem. Chem. Phys. 6 (2004) 11–22, https://doi.org/10.1039/B310395A.
[50] X. Li, B. Kiran, J. Li, H.-J. Zhai, L.-S. Wang, Experimental observation and confirmation of icosahedral $W@Au_{12}$ and $Mo@Au_{12}$ molecules, Angew. Chem. Int. Ed. Engl. 41 (2002) 4786–4789, https://doi.org/10.1002/anie.200290048.